The promoted synthesis of minoxidil by magnetic nanoparticles of cobalt ferrite (CoFe$_2$O$_4$) as a heterogeneous reusable catalyst

Ronak EISAVI[1] , **Fatemeh AHMADI**[1] , **Behzad ZEYNIZADEH**[2] , **Mehri KOUHKAN**[3,*]

[1]Department of Chemistry, Payame Noor University, Tehran, Iran
[2]Faculty of Chemistry, Urmia University, Urmia, Iran
[3]Department of Pharmacy, Urmia University of Medical Sciences, Urmia, Iran

Abstract: Minoxidil (2,4-diamino-6-piperidinopyrimidine 3-oxide) was primarily recognized as a drug for reducing vascular resistance to blood flow. It was later introduced as a more important medicine for topical stimulation of hair growth and baldness reverting as well as treatment of androgenic alopecia through increasing prostaglandin endoperoxide synthesis. In this study, magnetic nanoparticles (MNPs) of spinel ferrites (MFe$_2$O$_4$, M = Co, Ni, Fe, Cu, and Zn) via solid-state grinding procedure were prepared and then characterized using X-ray diffraction, scanning electron microscopy, transmission electron microscopy, vibrating sample magnetometer, and Fourier transform infrared techniques. The prepared nanoferrites were utilized as efficient and green heterogeneous catalysts for N-oxidation of 2,6-diamino-4-chloro-pyrimidine with H$_2$O$_2$ in refluxing ethanol giving 2,6-diamino-4-chloro-pyrimidine N-oxide as a starting material for the synthesis of 2,4-diamino-6-piperidinopyrimidine 3-oxide (minoxidil). Among the examined nanoferrites, CoFe$_2$O$_4$ MNPs exhibited prominent catalytic activity giving the product in 95% yield within 60 min. Moreover, the reusability of nano-CoFe$_2$O$_4$ was examined for 6 consecutive cycles without significant loss of catalytic activity and magnetic property.

Key words: Androgenic, Cobalt ferrite, Hydrogen peroxide, magnetic nanoparticles, minoxidil, solid-state

1. Introduction

Minoxidil was primarily recognized as an effective antihypertensive and peripheral vasodilator drug for reducing vascular resistance to blood flow [1,2]. However, it was later introduced as a more important medicine for topical stimulation of hair growth [3], baldness reverting [4], and treatment of androgenic alopecia through increasing prostaglandin endoperoxide synthesis [5]. Recently, magnetic nanoparticles of ferrites have been widely used as green and efficient heterogeneous catalysts in the synthesis of organic compounds. These NPs provide prominent advantages such as simple synthetic procedure, high catalytic activity due to huge surface area to volume ratio [6], chemical reactivity and thermal stability [7,8], easy separation using an external magnetic field without utilizing further traditional filtration process and perfect reusability [9,10]. Moreover, they have received a considerable interest because of their wide useful capabilities in drug delivery, magnetic resonance imaging, and biomedical technology [11–16]. It is notable that in pharmaceutical industry, the recovery and complete separation of magnetic nanocatalysts is important, because the presence of residual metals in final products may have dangerous consequences.

The development and characterization of nanoferrites have been quite significant to meet a number of

---

*Correspondence: mehrikouhkan@gmail.com

scientific and technological requirements especially in environmental and medical issues. Ferrites have been developed using different methods such as coprecipitation [17], hydrothermal [18], and solid-state [19]. Among these methods, solid-state procedure is a facile approach with great economic and technical advantages to obtain highly crystalline nanoparticles.

As a part of our research program on the synthesis of nanomagnetic materials and their application in functional group transformations [20–22], herein, we wish to introduce nanospinel ferrites as efficient and reusable heterogeneous catalysts for N-oxidation of 6-chloro-2,4-diaminopyrimidine to 2,6-diamino-4-chloro-pyrimidine N-oxide by H_2O_2 in ethanol under reflux conditions. Then, through the nucleophilic reaction of piperidine with 2,6-diamino-4-chloro-pyrimidine N-oxide, minoxidil (2,4-diamino-6-piperidino-pyrimidine 3-oxide) was produced in high yield and purity (Figure 1).
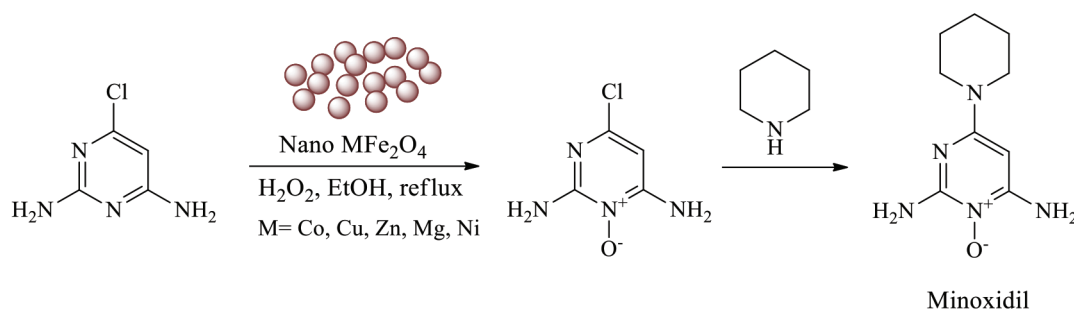
Figure 1. Synthesis of minoxidil.

2. Experimental

2.1. General

All reagents and materials were purchased from Merck and Aldrich chemical companies with high quality and used without further purification. Scanning electron microscopy (SEM) images of NPs were recorded on FESEM-TESCAN. TEM images were recorded on Philips CM30 at electron energy at 300 KeV. Characterization of nanocatalysts were carried out by X-Ray diffraction (XRD) using a Bruker D8-Advanced diffractometer with graphite-monochromatized Cu Kα radiation (λ=1.54056 Å) at room temperature. Magnetic properties of nanoferrites were measured using a vibrating sample magnetometer (VSM, Meghnatis Daghigh Kavir Co., Iran) at room temperature. Fourier transform infrared (FT-IR) and ^{1}H/^{13}C NMR spectra were recorded on Thermo Nicolet Nexus 670 FT-IR and 500 MHz Bruker Avance spectrometers, respectively. Products were identified through spectral analysis and then compared with authentic data in the literature. All yields refer to isolated pure products.

2.2. Preparation of CoFe$_2$O$_4$ magnetic nanoparticles

Magnetic nanoparticles (MNPs) of CoFe$_2$O$_4$ were prepared through a solid-state grinding procedure. In an agate mortar, a mixture of CoCl$_2$, Fe(NO$_3$)$_3 \cdot$9H$_2$O, NaOH, and NaCl in a molar ratio of 1:2:8:2 was prepared and then ground for 45 min at room temperature. The reaction was started with the release of heat and the change of color from yellow to dark brown after 4 min. After the reaction was completed (45 min), the excess amount of salt was removed from the reaction mixture through washing with distilled water. The obtained residue was dried in an oven at 80 °C for 60 min. The resulting powder was smoothly calcinated at 300,

500, 700, and 900 °C within 80 min (20 min at each temperature) affording $CoFe_2O_4$ MNPs. Consequently, $MgFe_2O_4$, $NiFe_2O_4$, $ZnFe_2O_4$, and $CuFe_2O_4$ MNPs were prepared through similar procedure and then characterized (supplementary information).

2.3. Synthesis of 2,6-diamino-4-chloro-pyrimidine *N*-oxide

In a two-neck round-bottom flask equipped with magnetic stirrer and condenser, a mixture of 2,6-diamino-4-chloro-pyrimidine (1 mmol, 0.14 g) and $CoFe_2O_4$ MNPs (0.01 g, 0.05 mmol, 5 mol%) in EtOH (5 mL) was placed. The mixture was stirred for 1 min at 40 °C, and then H_2O_2 (30%, 0.5 mL) was added dropwise into the reaction mixture. The resulting mixture was then magnetically stirred under reflux conditions for 60 min. Progress of the reaction was monitored by thin layer chromotography (TLC) [eluent: $CHCl_3$:MeOH:EtOAc (5:4:1)]. After the completion of reaction, the mixture was cooled to room temperature and MNPs of $CoFe_2O_4$ were separated from the reaction mixture using an external magnetic field. The final product was filtered and washed with ethanol, recrystallized from hot water and dried in oven at 80 °C affording 2,6-diamino-4-chloro-pyrimidine *N*-oxide as a white solid (95% yield, 0.15 g, mp. 189 °C). ^{1}H NMR (d_6-DMSO) δ (ppm) 7.57 (bs, 4H, $2NH_2$), 6.09 (s, 1H, Ar-H); ^{13}CNMR (d_6-DMSO) δ (ppm) 153.76, 153.52, 145.34, 92.52; FT-IR (ν_{max}, cm^{-1}, neat) 3473, 3415, 3339, 3284, 3143, 1618, 1567, 1483, 1372, 1205, 1158, 922, 795, 767, 736, 651, 611, 539, 530, 505.

2.4. Synthesis of 2,4-diamino-6-piperidinopyrimidine 3-oxide (minoxidil)

In a round-bottom flask equipped with magnetic stirrer and condenser, a mixture of piperidine (1.8 mL, 1.55 g, 18.2 mmol) and 2,6-diamino-4-chloro-pyrimidine *N*-oxide (0.16 g, 1 mmol) was placed and then stirred in boiling piperidine (106 °C) for 120 min. Progress of the reaction was monitored by TLC. After the reaction was completed, the excess amount of piperidine was removed by evaporation under reduced pressure. The resulting solid material was washed with water, recrystallized from hot water affording minoxidil as a colorless crystalline solid (80% yield, 0.17g, mp. 258?260 °C). ^{1}H NMR (d_6-DMSO) δ (ppm) 6.83 (bs, 4H, $2NH_2$), 5.35 (s, 1H, Ar-H), 3.36 (t, $J = 5.32$ Hz, 4H, $2CH_2$-N), 1.62-1.44 (m, 6H, $3CH_2$); ^{13}C NMR (d_6-DMSO) δ (ppm) 155.52, 153.47, 152.27, 73.52, 45.39, 25.36, 24.58; FT-IR (ν_{max}, cm^{-1}, neat) 3307, 2932, 2853, 2261, 2140, 1651, 1611, 1475, 1445, 1374, 1287, 1249, 1228, 1150, 1124, 1083, 1023, 1004, 876, 820, 761, 481.

3. Results and discussions
3.1. Preparation of $CoFe_2O_4$ MNPs

MNPs of $CoFe_2O_4$ were synthesized through solid-state grinding of $CoCl_2$, $Fe(NO_3)_3 \cdot 9H_2O$, NaCl, and NaOH in a molar ratio of 1:2:8:2 (Figure 2). The resulting dark brown residue was washed, dried, and then calcinated at 300–900 °C. The prepared $CoFe_2O_4$ MNPs were then characterized using XRD, vibrating sample magnetometer (VSM), SEM, transmission electron microscopy (TEM), and FT-IR techniques.
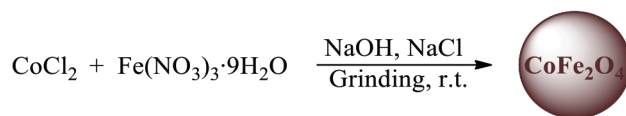

Figure 2. Synthesis of $CoFe_2O_4$ MNPs.

3.2. Characterization of $CoFe_2O_4$ MNPs

3.2.1. X-Ray Diffraction (XRD)

Figure 3 displays XRD pattern of $CoFe_2O_4$ MNPs. The pattern showed the reflection planes of (3 1 1), (4 4 0), and (5 1 1) corresponding to $2\theta = 35.57°$, $62.71°$ and $57.12°$, respectively. Comparison of the obtained patterns with standard data (JCPDS card no. 22-1086) exhibited that the laboratory sample of $CoFe_2O_4$ had high phase purity and crystallinity. Moreover, the average crystal size of $CoFe_2O_4$ using Scherrer equation was calculated to be 66 nm [23].
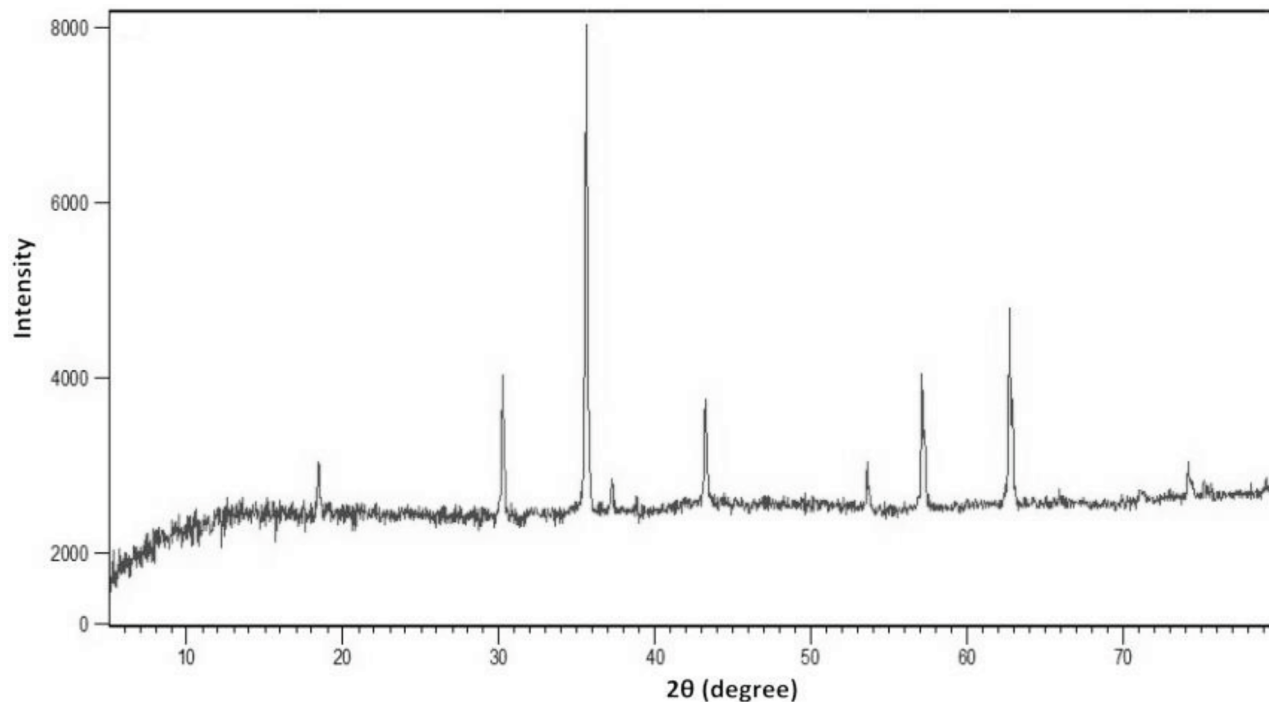
Figure 3. XRD pattern of $CoFe_2O_4$ MNPs.

3.2.2. Vibrating sample magnetometer (VSM)

Figure 4 shows the magnetic property of $CoFe_2O_4$ MNPs which was plotted using a VSM instrument under an external magnetic field of up to 20 kOe. It has been reported that the magnetization saturation value (Ms) of a nanomaterial is a direct function of its dimensions, such that by increase of the agglomeration and size of NPs, Ms value is also increased [24]. The shape of magnetization curve verfied that $CoFe_2O_4$ MNPs behaved as hard ferromagnetic materials [25]. Moreover, it was shown that Ms value and coercivity of $CoFe_2O_4$ MNPs were 128 emu g$^{?1}$ and 800 Oe, respectively.

3.2.3. Scanning electron microscopy (SEM)

Morphology of the surface of $CoFe_2O_4$ MNPs was investigated using SEM technique (Figure 5). SEM images demonstrated that agglomeration of NPs occurred to some extent affording spherical segments with diameters 64-66 nm.
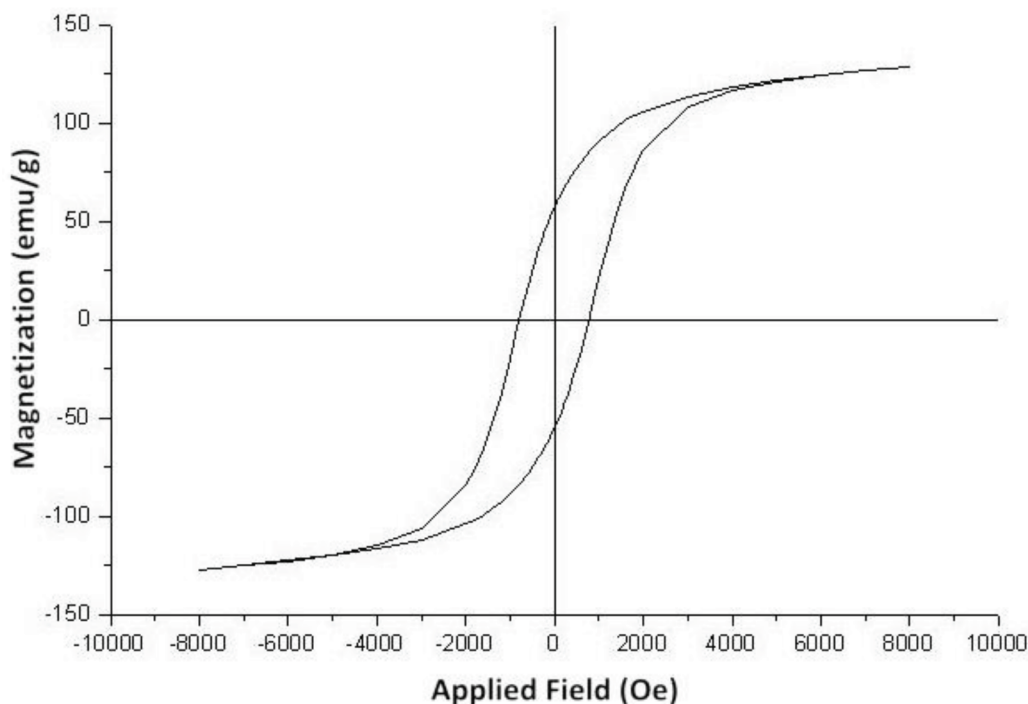
Figure 4. Magnetization curve of $CoFe_2O_4$ MNPs.

3.2.4. Fourier transform infrared spectroscopy (FT-IR)

FT-IR spectrum of $CoFe_2O_4$ MNPs is shown in Figure 6. The spectrum represents a strong absorption band at 576 cm^{-1} corresponding to stretching vibration of metal-oxygen (M-O) bond indicating the formation of spinal ferrite structure. The absorption peaks at 1616 and 3430 cm^{-1} are also attributed to bending and stretching vibrations of O-H groups on the surface of $CoFe_2O_4$ MNPs and the adsorbed water by sample, respectively [26]. The latter absorption signal for adsorbed water could be weakened by the calcination of NPs.

3.3. Synthesis of minoxidil

Minoxidil was synthesized in a two-step procedure: i) N-oxidation of 2,6-diamino-4-chloro-pyrimidine and ii) preparation of 2,4-diamino-6-piperidinopyrimidine 3-oxide through the reaction of piperidine with 2,6-diamino-4-chloro-pyrimidine N-oxide (Figure 7).

3.3.1. Preparation of 2,6-diamino-4-chloro-pyrimidine N-oxide

Synthesis of 2,6-diamino-4-chloro-pyrimidine N-oxide was carried out via N-oxidation of 6-chloro-2,4-diaminopyrimidine with H_2O_2 in the presence of various magnetic nanocatalysts ($CoFe_2O_4$, $MgFe_2O_4$, $CuFe_2O_4$, $NiFe_2O_4$ and $ZnFe_2O_4$) under different reaction conditions including the change of quantities of nanocatlysts and hydrogen peroxide, temperature and reaction solvent. The results of this investigation are summarized in Table. Observation of the results represented that N-oxidation of 6-chloro-2,4-diaminopyrimidine with H_2O_2 in the absence of any nanoferrite catalyst did not proceed. However, using a small amount of spinel ferrites dramatically affected N-oxidation of pyrimidine ring. More examinations also exhibited that among various nanospinel ferrites, $CoFe_2O_4$ MNPs showed excellent catalytic activity. In addition, using 5 mol% of $CoFe_2O_4$ and 0.5
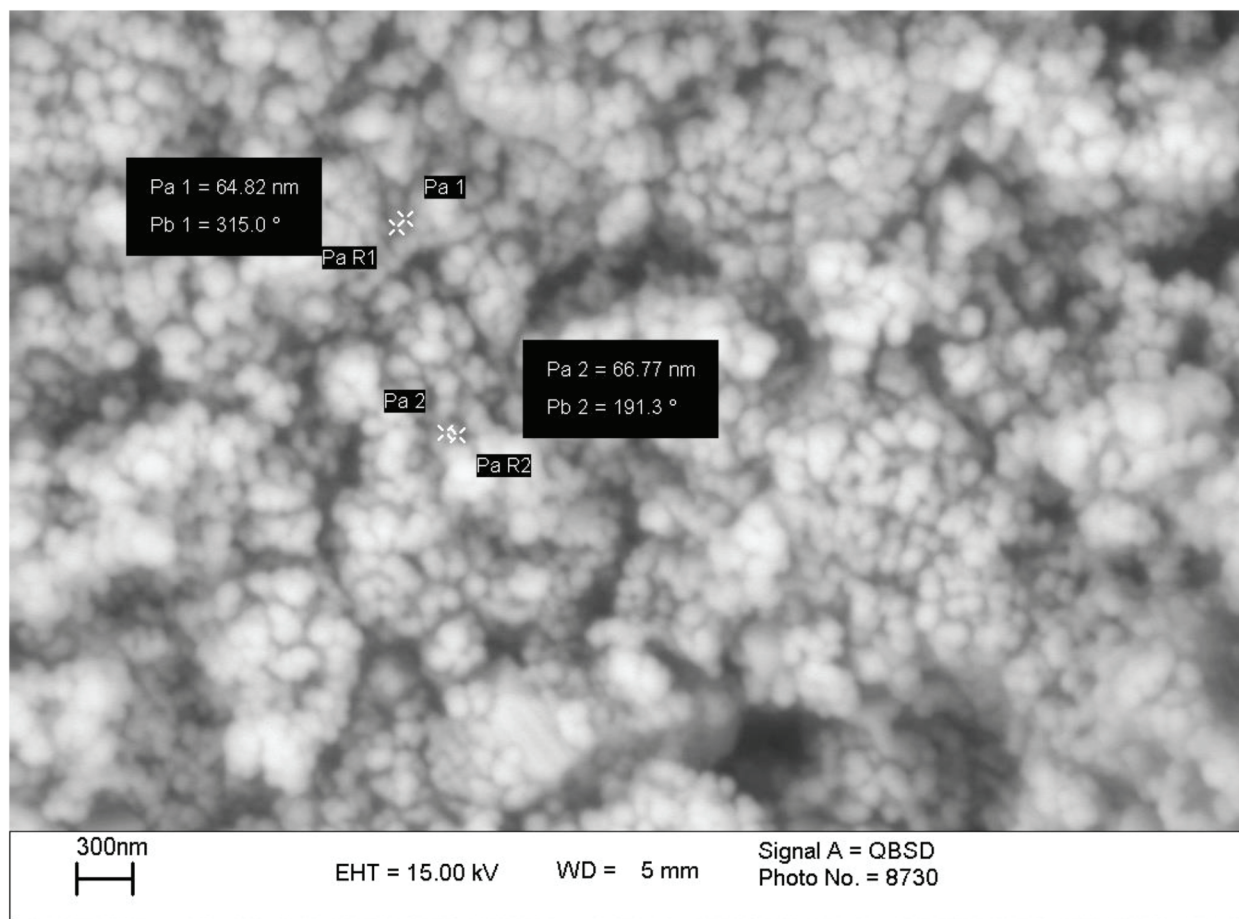
Figure 5. SEM image of $CoFe_2O_4$ MNPs.

mL of H_2O_2 per 1 mmol of 6-chloro-2,4-diaminopyrimidine in ethanol under reflux conditions (entry 6, Table) were the optimum requirements for the completion of reaction.

The green aspect of this methodology was also studied through the reusability investigation of the applied $CoFe_2O_4$ towards N-oxidation of 6-chloro-2,4-diaminopyrimidine with H_2O_2 under optimized reaction conditions. In this context, when the reaction of N-oxidation was completed, the nanocatalyst was recovered from the reaction mixture using an external magnetic field. After washing with EtOAc and drying in an oven, the vessel of N-oxidation reaction was charged with fresh 6-chloro-2,4-diaminopyrimidine, H_2O_2 and the recovered $CoFe_2O_4$ for a second run. Figure 8 clearly shows that $CoFe_2O_4$ MNPs could be reused for 6 consecutive cycles without significant loss of its catalytic activity and magnetic property.

3.3.2. Synthesis of 2,4-diamino-6-piperidinopyrimidine 3-oxide

2,4-Diamino-6-piperidinopyrimidine 3-oxide (minoxidil) was successfully synthesized from the nucleophilic substitution reaction of piperidine with 2,6-diamino-4-chloro-pyrimidine N-oxide in boiling piperidine (106 °C) under neat conditions. The reaction was completed within 120 min affording minoxidil product in high yield (80 %) and purity without requiring any further purification. Minoxidil was in a tautomeric equilibrium with 6-amino-1,2-dihydro-1-hydroxy-2-imino-4-piperidinylpyrimidine (Figure 7).
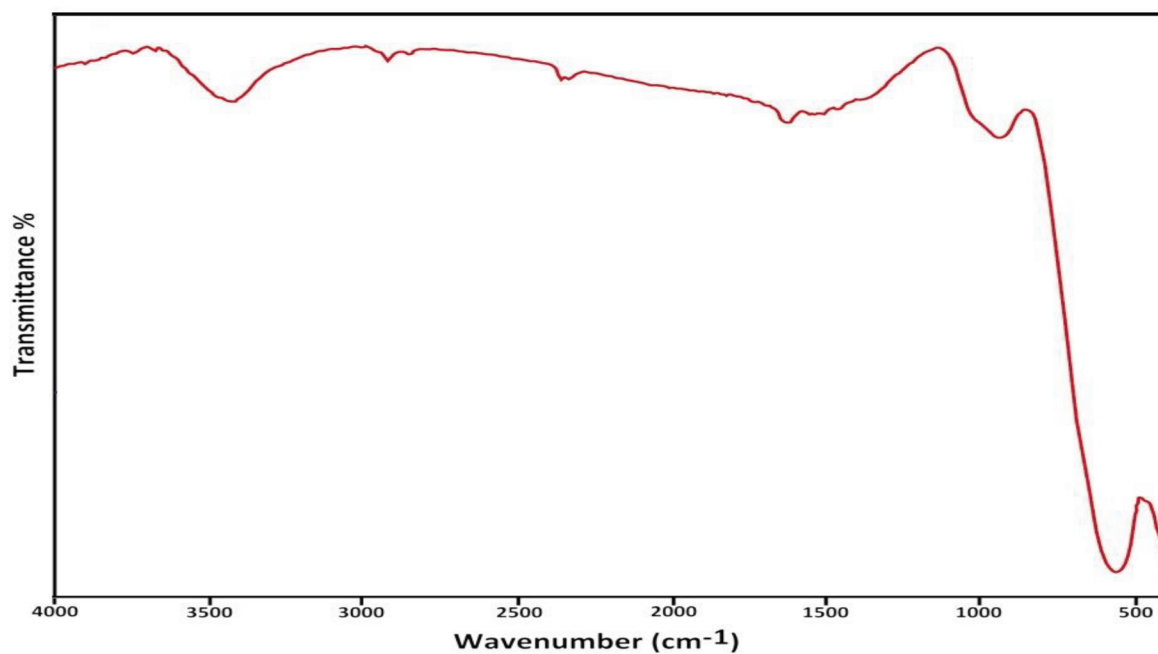
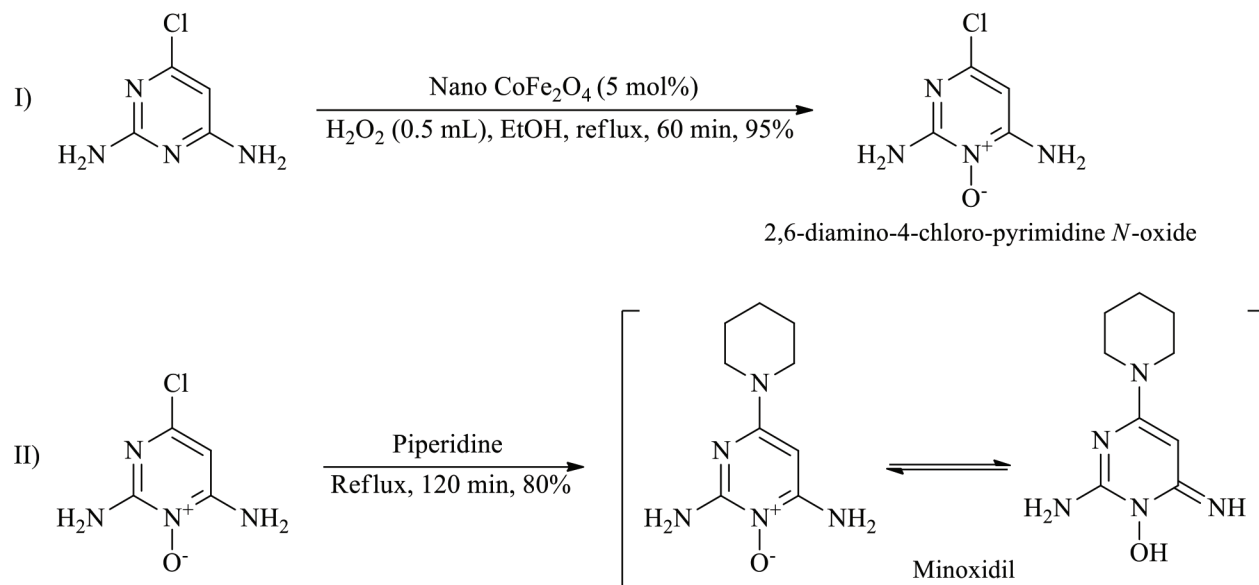**Figure 6**. FT-IR spectrum of $CoFe_2O_4$ MNPs.

Figure 7. Two-step procedure for synthesis of minoxidil.

Although the exact mechanism of this synthetic protocol is not clear, the mechanism depicted in Figure 9 shows the role of nanocatalyst in promoting the synthesis of minoxidil in a two-step procedure. The figure shows that due to the Lewis acidity of transition metals existing in spinel ferrites, 6-chloro-2,4-diaminopyrimidine interacted with the surafce of nanocatalyst [27-32]. Then, by the addition of H_2O_2 and its interaction with the surface of nanocatalyst, N-oxidation of pyrimidine ring was carried out giving 2,6-diamino-4-chloro-pyrimidine N-oxide. Next, through the nucelophic attack of piperidne with 2,6-diamino-4-chloro-pyrimidine N-oxide, minoxidil product was successfully produced.

**Table 1.** Nano MFe_2O_4 catalyzed N-oxidation of 6-chloro-2,4-diaminopyrimidine with H_2O_2 under different conditions[a].

Entry	Catalyst (mol%)	H_2O_2 (mL)	Conditions	Time (min)	Conversion (%)[b]	Yield (%)
1	-	0.5	EtOH/reflux	60	0	0
2	$CuFe_2O_4$ (5 mol%)	0.5	EtOH/reflux	90	100	80
3	$NiFe_2O_4$ (5 mol%)	0.5	EtOH/reflux	100	100	85
4	$MgFe_2O_4$ (5 mol%)	0.5	EtOH/reflux	120	100	85
5	$ZnFe_2O_4$ (5 mol%)	0.5	EtOH/reflux	130	100	70
6	$CoFe_2O_4$ (5 mol%)	0.5	EtOH/reflux	60	100	95
7	$CoFe_2O_4$ (3 mol%)	0.5	EtOH/reflux	90	100	90
8	$CoFe_2O_4$ (10 mol%)	0.5	EtOH/reflux	55	100	95
9	$CoFe_2O_4$ (5 mol%)	0.1	EtOH/reflux	150	100	80
10	$CoFe_2O_4$ (5 mol%)	0.3	EtOH/reflux	90	100	85
11	$CoFe_2O_4$ (5 mol%)	0.7	EtOH/reflux	60	100	94
12	$CoFe_2O_4$ (5 mol%)	0.5	MeOH/reflux	60	100	90
13	$CoFe_2O_4$ (5 mol%)	0.5	H_2O/reflux	240	10	-
14	$CoFe_2O_4$ (5 mol%)	0.5	CH_3CN/reflux	360	50	-
15	$CoFe_2O_4$ (5 mol%)	0.5	$CHCl_3$/reflux	240	20	-
16	$CoFe_2O_4$ (5 mol%)	0.5	EtOH/r.t.	60	0	?
17	$CoFe_2O_4$ (5 mol%)	0.5	Solvent-free, 70 °C	60	100	80

[a] All reactions were carried out with 1 mmol of 6-chloro-2,4-diaminopyrimidine. [b] Conversion less than 100% was determined on the basis of the recovered 6-chloro-2,4-diaminopyrimidine.
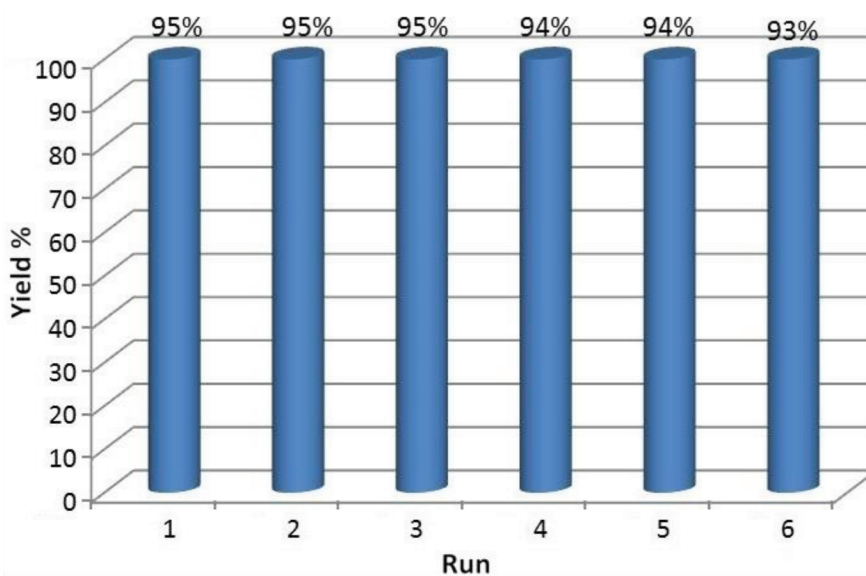
Figure 8. Reusability of $CoFe_2O_4$ MNPs in N-oxidation of 6-chloro-2,4-diaminopyrimidine.I) N-oxidation of 2,6-diamino-4-chloro-pyrimidine II) Nucleophilic reaction of piperidine on 2,6-diamino-4-chloro-pyrimidine N-oxide
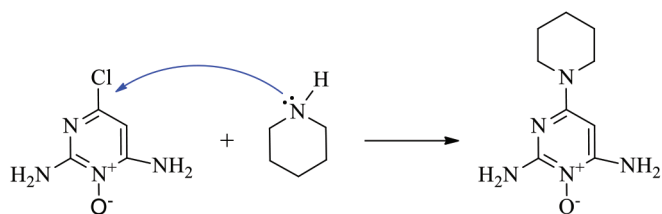
II) Nucleophilic reaction of piperidine on 2,6-diamino-4-chloro-pyrimidine *N*-oxide

Figure 9. A proposed mechanism for synthesis of mioxidil catalyzed by $CoFe_2O_4$ MNPs.

4. Conclusion

In this study, we have introduced an easy protocol for the synthesis of minoxidil drug by the reaction of piperidine with 2,6-diamino-4-chloro-pyrimidine *N*-oxide under neat conditions. 2,6-Diamino-4-chloro-pyrimidine *N*-oxide was primarily synthesized from *N*-oxidation of 6-chloro-2,4-diaminopyrimidine using H_2O_2 in the presence of $CoFe_2O_4$ magnetic nanocatalyst in ethanol under reflux conditions. The effect of other magnetic nanocatalysts such as $CuFe_2O_4$, $NiFe_2O_4$, $MgFe_2O_4$, and $ZnFe_2O_4$ was also investigated. Based on the obtained results, the current protocol had prominent advantages in terms of cost-effectiveness, easy synthesis, and great reusability of the magnetic nanocatalyst, as well as magnetic separation of the catalyst instead of using traditional filtration process, short reaction time, and high yield of final product.

Acknowledgment

References

1. Meisheri KD, Cipkus LA, Taylor CJ. Mechanism of action of minoxidil sulfate-induced vasodilation: a role for increased K^+ permeability. Journal of Pharmacology and Experimental Therapeutics 1988; 245 (3): 751-760.

2. Winquist RJ, Heaney LA, Wallace AA, Baskin EP, Stein RB et al. Glyburide blocks the relaxation response to BRL 34915 (cromakalim), minoxidil sulfate and diazoxide in vascular smooth muscle. Journal of Pharmacology and Experimental Therapeutics 1989; 248 (1): 149-156.

3. Proctor PH. Endothelium-derived relaxing factor and minoxidil: active mechanisms in hair growth. Archives of Dermatology 1989; 125 (8): 1146. doi: 10.1001/archderm.1989.01670200122026

4. Ellis JA, Sinclair RD. Male pattern baldness: current treatments, future prospects. Drug Discovery Today 2008; 13 (17-18): 791-797. doi: 10.1016/j.drudis.2008.05.010

5. Gorecki DKJ. Minoxidil. Analytical Profiles of Drug Substances 1988; 17: 185-219. doi: 10.1016/S0099-5428(08)60220-8

6. Zhang Z, Liu Y, Yao G, Guoyin Z, Hao Y. Synthesis and characterization of $NiFe_2O_4$ nanoparticles via solid-state reaction. International Journal of Applied Ceramic Technology 2013; 10 (1): 142-149. doi: 10.1111/j.1744-7402.2011.02719.x

7. Lu AH, Salabas EL, Schuth F. Magnetic nanoparticles: synthesis, protection, functionalization, and application. Angewandte Chemie International Edition 2007; 46 (8): 1222-1244. doi: 10.1002/anie.200602866

8. Zhu Y, Stubbs LP, Ho F, Liu R, Ship CP et al. Magnetic nanocomposites: a new perspective in catalysis. ChemCatChem 2010; 2 (4): 365-347. doi:10.1002/cctc.200900314

9. Lim CW, Lee IS. Magnetically recyclable nanocatalyst systems for the organic reactions. Nanotoday 2010; 5 (5): 412-434. doi: 10.1016/j.nantod.2010.08.008

10. Gawande M, Rathi A, Branco P, Varma RS. Sustainable utility of magnetically recyclable nanocatalysts in water: applications in organic synthesis. Applied Sciences 2013; 3 (4): 656-674. doi: 10.3390/app3040656

11. Gupta AK, Gupta M. Synthesis and surface engineering of iron oxide nanoparticles for biomedical applications. Biomaterials 2005; 26 (18): 3995-4021. doi: 10.1016/j.biomaterials.2004.10.012

12. Chen D, Zeng D, Liu Z. Synthesis, structure, morphology evolution and magnetic properties of single domain strontium hexaferrite particles. Materials Research Express 2016; 3 (4): 045002. doi: 10.1088/2053-1591/3/4/045002

13. Mornet S, Vasseur S, Grasset F, Veverka P, Goglio G et al. Magnetic nanoparticle design for medical applications. Progress in Solid State Chemistry 2006; 34 (2-4): 237-247. doi: 10.1016/j.progsolidstchem.2005.11.010

14. Chen D, Meng Y, Gandha KH, Zeng D, Yu H et al. Morphology control of hexagonal strontium ferrite micro/nano-crystals. American Institute of Physics Advances 2017; 7 (5): 056214. doi: 10.1063/1.4974283

15. Hyeon T, Lee SS, Park J, Chung Y, Na HB. Synthesis of highly crystalline and mono disperse maghemite nanocrystallites without a size-selection process. Journal of the American Chemical Society 2001; 123 (51): 12798-12801. doi: 10.1021/ja016812s

16. Pullar RC. Hexagonal ferrites: A review of the synthesis, properties and applications of hexaferrite ceramics. Progress in Materials Science 2012; 57 (7): 1191-1334. doi: 10.1016/j.pmatsci.2012.04.001

17. Kashid P, Mahadev S, Kulkarni AB, Mathad SN, Shedam R. Synthesis and structural studies of nano $Co_{0.85}Cd_{0.15}$ Fe_2O_4 ferrite by co-precipitation method. Journal of Advanced Physics 2017; 6 (4): 545-548. doi: 10.1166/jap.2017.1373

18. Zhang D, Zhang X, Ni X, Song J, Zheng H. Low-temperature fabrication of $MnFe_2O_4$ octahedrons: magnetic and electrochemical properties. Chemical Physics Letters 2006; 426 (1-3): 120-123. doi: 10.1016/j.cplett.2006.05.100

19. Hassanzadeh S, Eisavi R, Abbasian M. Preparation and characterization of magnetically separable $MgFe_2O_4$ /$Mg(OH)_2$ nanocomposite as an efficient heterogeneous catalyst for regioselective one-pot synthesis of β - chloroacetates from epoxides. Applied Organometallic Chemistry 2018; 32 (11): e4520. doi: 10.1002/aoc.4520

20. Eisavi R, Ghadernejad S, Zeynizadeh B, Mohammad Aminzadeh F. Magnetically separable nano $CuFe_2O_4$: an ef?cient and reusable heterogeneous catalyst for the green synthesis of thiiranes from epoxides with thiourea. Journal of Sulfur Chemistry 2016; 37 (5): 537-545. doi: 10.1080/17415993.2016.1196691

21. Eisavi R, Ahmadi F, Ebadzade B, Ghadernejad S. A green method for solvent-free conversion of epoxides to thiiranes using NH_4SCN in the presence of $NiFe_2O_4$ and $MgFe_2O_4$ magnetic nanocatalysts. Journal of Sulfur Chemistry 2017; 38 (6): 614-624. doi: 10.1080/17415993.2017.1334780

22. Eisavi R , Alifam S. $ZnFe_2O_4$ nanoparticles: A green and recyclable magnetic catalyst for fast and regioselective conversion of epoxides to vicinal hydroxythiocyanates using NH_4SCN under solvent-free conditions. Phosphorus, Sulfur, and Silicon and the Related Elements 2018; 193 (4): 211-217. doi: 10.1080/10426507.2017.1390460

23. Lida H, Takayannagi K, Nakamishi T, Osaka T. Synthesis of Fe_3O_4 nanoparticles with various sizes and magnetic properties by controlled hydrolysis. Journal of Colloid and Interface Science 2007; 314 (1): 274-280. doi: 10.1016/j.jcis.2007.05.047

24. Sanchez RD, Rivas J, Vaqueiro P, Lopez-Quintela MA, Caeiro D. Particle size effects on magnetic properties of yttrium iron garnets prepared by a sol–gel method. Journal of Magnetism and Magnetic Materials 2002; 247 (1): 92-98. doi: 10.1016/S0304-8853(02)00170-1

25. Mazario E, Herrasti P, Morales MP, Menendez N. Synthesis and characterization of $CoFe_2O_4$ ferrite nanoparticles obtained by an electrochemical method. Nanotechnology 2012; 23 (35): 355708. doi: 10.1088/0957-4484/23/35/355708

26. Sathiya S, Parasuraman K, Anbarasu M, Balamurugan K. FT-IR, XRD, and SEM study of $CoFe_2O_4$ nanoparticles by chemical co-precipitation method. Nano Vision 2015; 5 (4-6): 133-138.

27. Sharma VB, Jain SL, Sain B. Bromamine-T/$RuCl_3$ as an efficient system for the oxidation of tertiary amines to N-oxides. Tetrahedron Letters 2004; 45 (22): 4281-4283. doi: 10.1016/j.tetlet.2004.04.014

28. Ionescu R, Pavel OD, Bırjega R, Zavoianu R, Angelescu E. Epoxidation of cyclohexene with H_2O_2 and acetonitrile catalyzed by Mg–Al hydrotalcite and cobalt modified hydrotalcites. Catalysis Letters 2010; 134 (3-4): 309-317. doi: 10.1007/s10562-009-0238-y

29. Zhu Z, Espenson JH. Methylrhenium trioxide as a catalyst for oxidations with molecular oxygen and for oxygen transfer. Journal of Molecular Catalysıs A: Chemıcal 1995; 103 (2): 87-94. doi: 10.1016/1381-1169(95)00120-4.

30. Li Z, Gao J, Xing X, Wu S, Shuang S et al. Synthesis and characterization of n-alkylamine-stabilized palladium nanoparticles for electrochemical oxidation of methane. Journal of Physical Chemistry C 2010; 114 (2): 723-733. doi: 10.1021/jp907745v

31. Yamamoto M, Kashiwagi Y, Nakamoto M. Size-controlled synthesis of monodispersed silver nanoparticles capped by long-chain alkyl carboxylates from silver carboxylate and tertiary amine. Langmuir 2006; 22 (20): 8581-8586. doi: 10.1021/la0600245

32. Leger B, Denicourt-Nowicki A, Olivier-Bourbigou H, Roucoux A. Rhodium nanocatalysts stabilized by various bipyridine ligands in nonaqueous ionic liquids: effect of the bipyridine coordination modes in arene catalytic hydrogenation. Inorganic Chemistry 2008; 47 (19): 9090-9096. doi: 10.1021/ic8010713

FT-IR, ^{1}H/^{13}C NMR spectra of 2,6-diamino-4-chloro-pyrimidine *N*-oxide and minoxidil as well as VSM, SEM, TEM, XRD and FT-IR spectrum of $MgFe_2O_4$, $CuFe_2O_4$, $NiFe_2O_4$ and $ZnFe_2O_4$ were given in supplementary information.
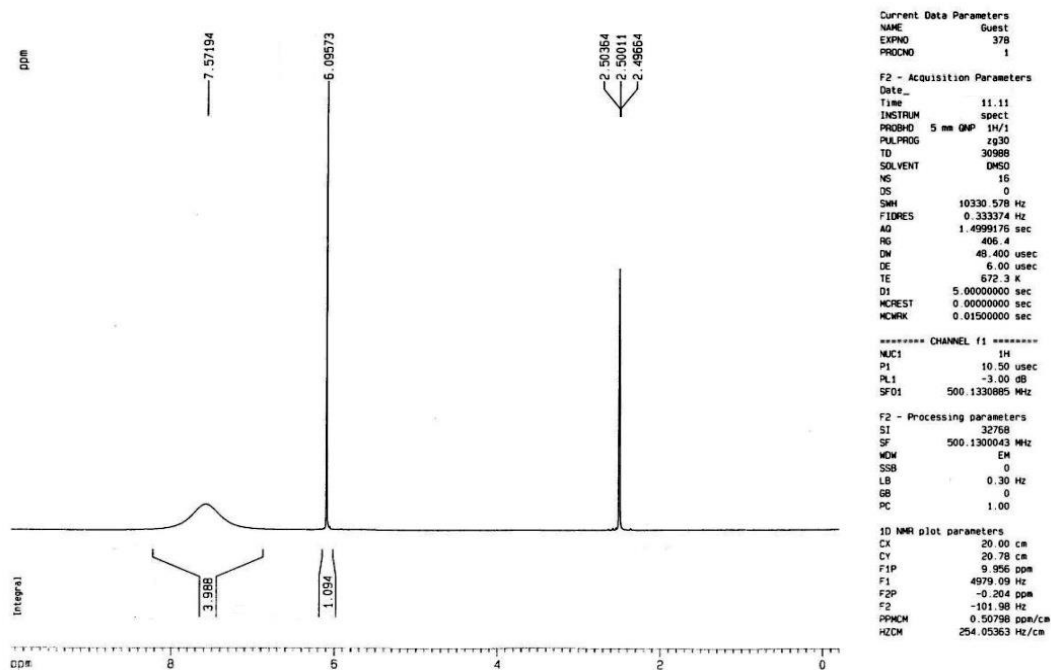
Figure S1. ^{1}H NMR spectrum of 2,6-diamino-4-chloro-pyrimidine *N*-oxide.
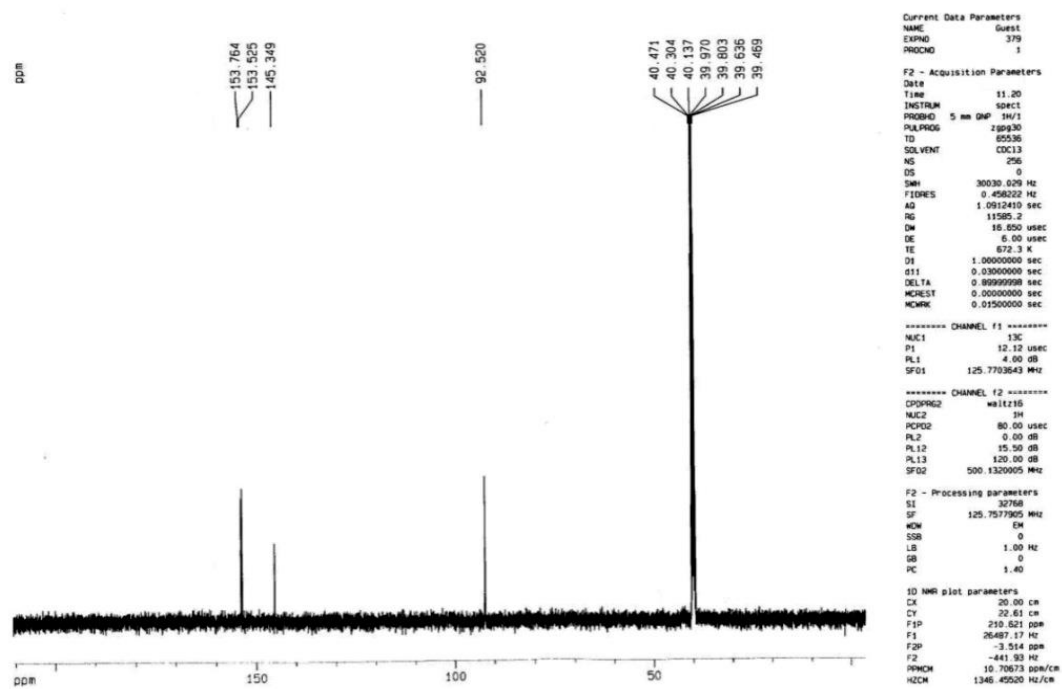
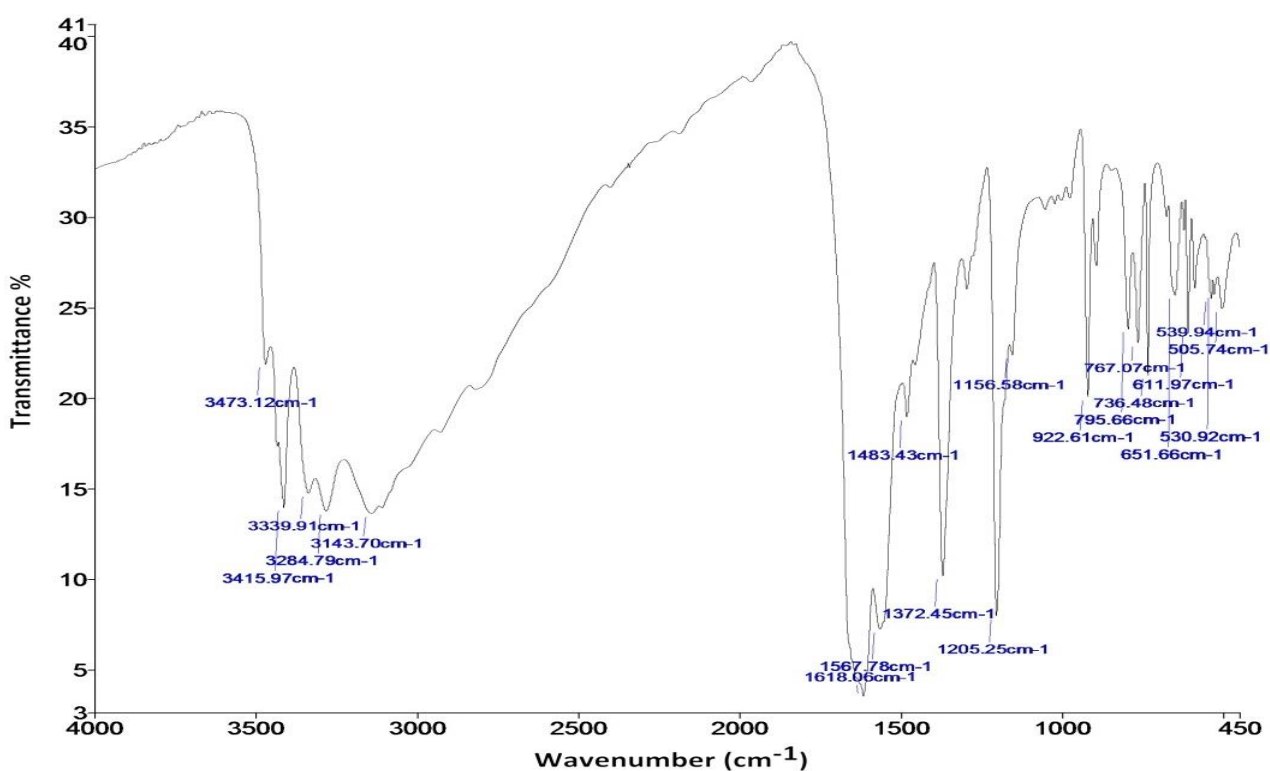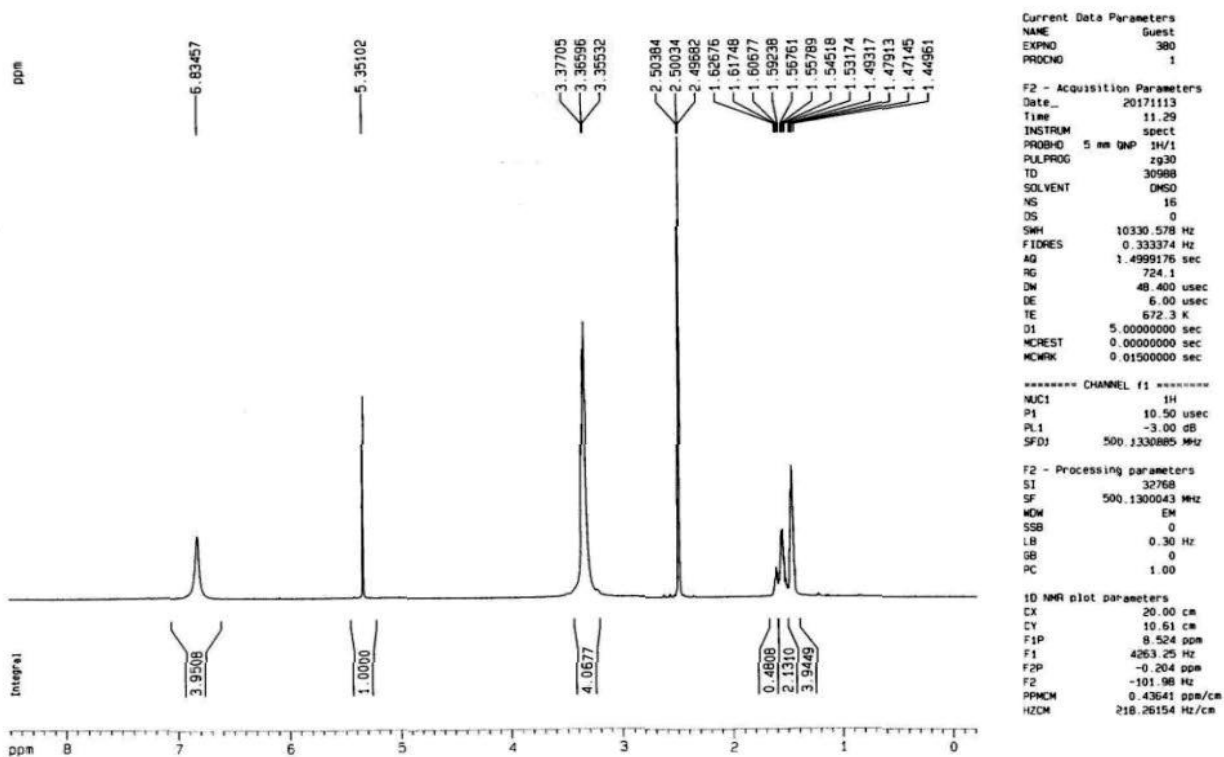**Figure S2.** ^{13}C NMR spectrum of 2,6-diamino-4-chloro-pyrimidine *N*-oxide.

Figure S3. FT-IR (KBr) spectrum of 2,6-diamino-4-chloro-pyrimidine *N*-oxide.

Figure S4. ¹H NMR spectrum of minoxidil.
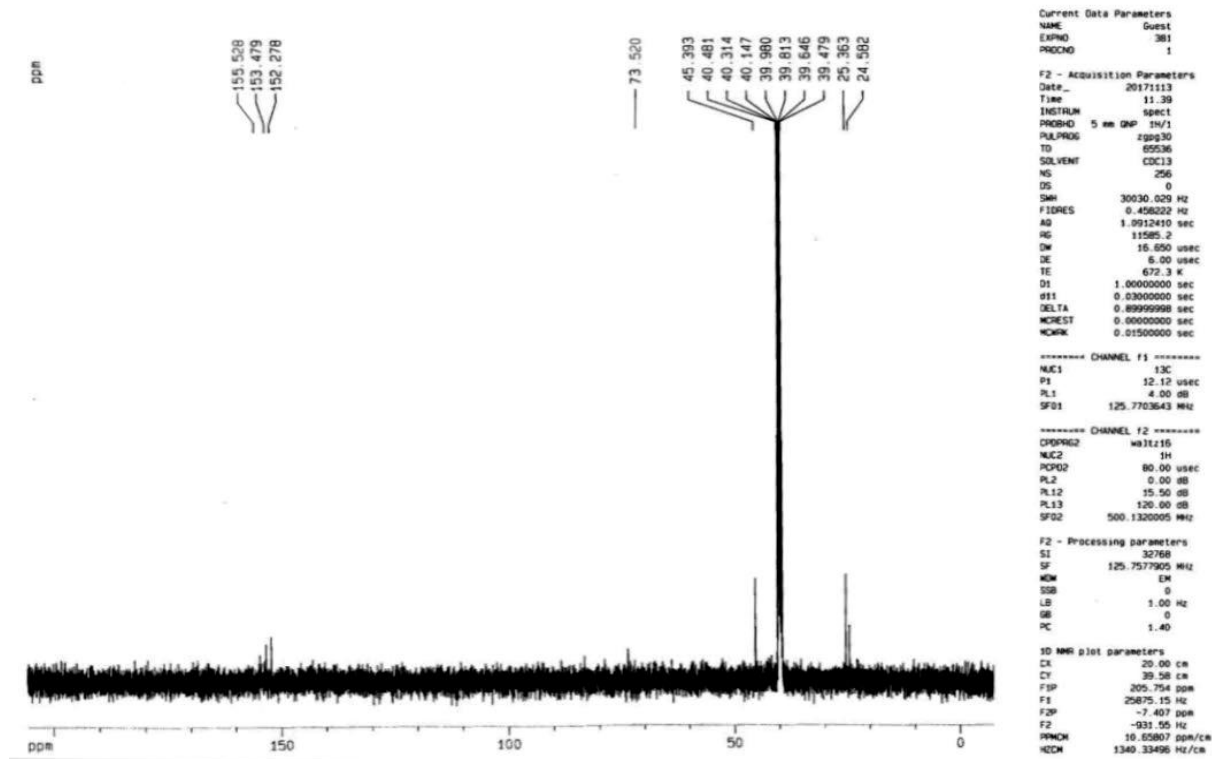
Figure S5. ^{13}C NMR spectrum of minoxidil.
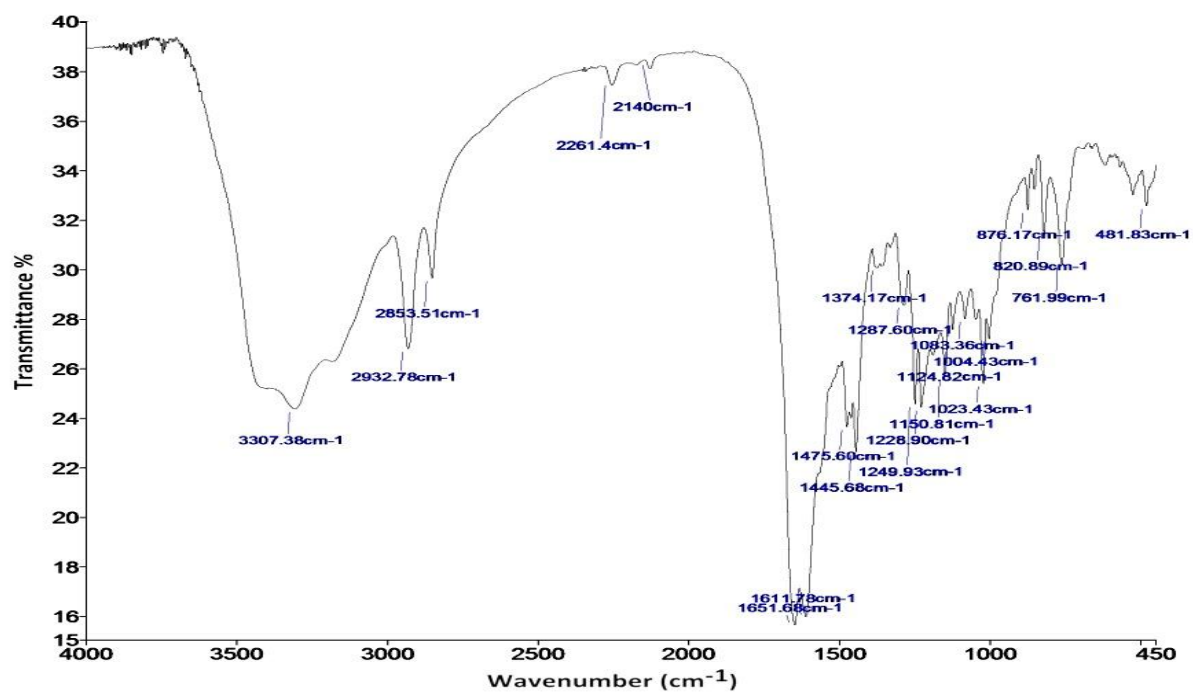
Figure S6. FT-IR (KBr) spectrum of minoxidil.
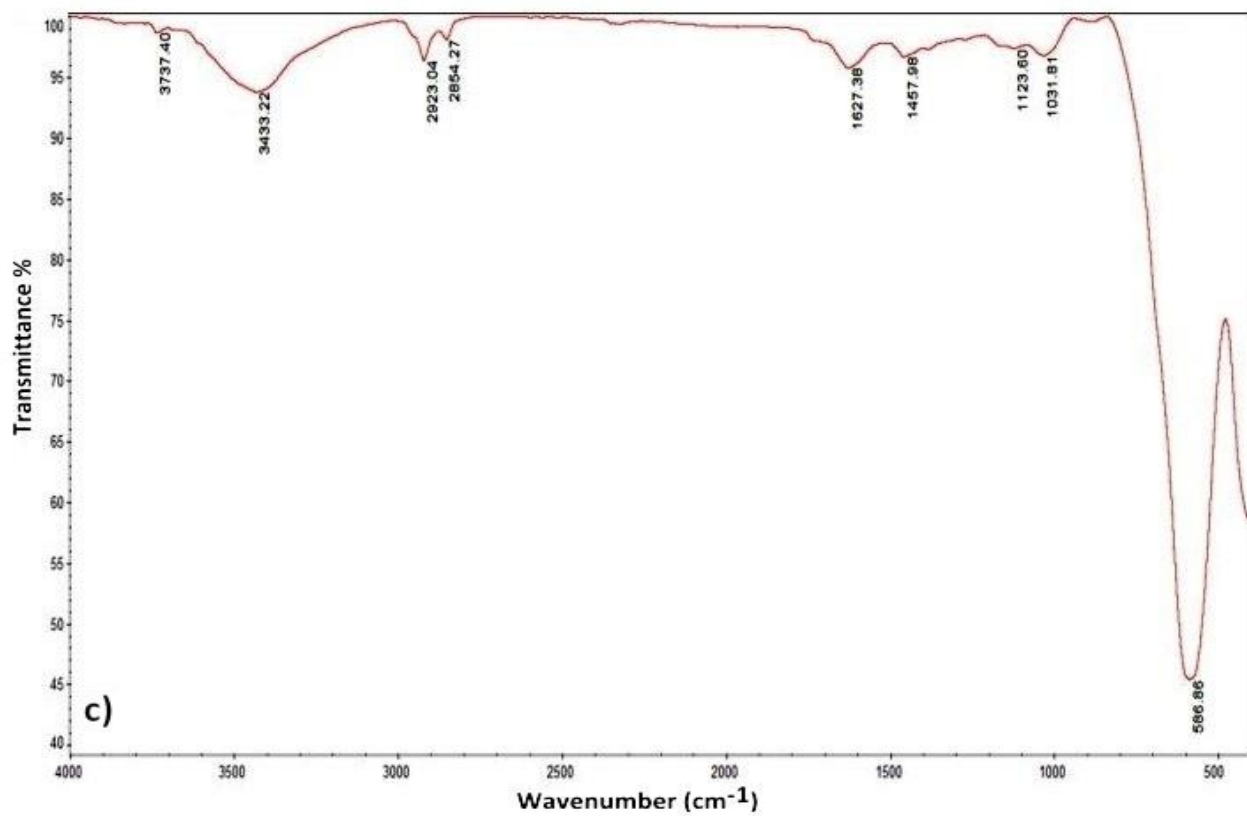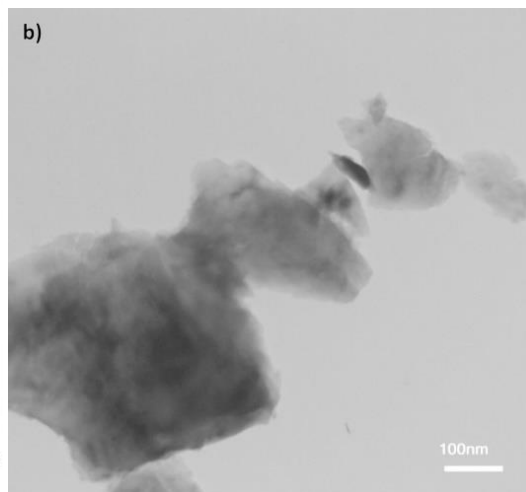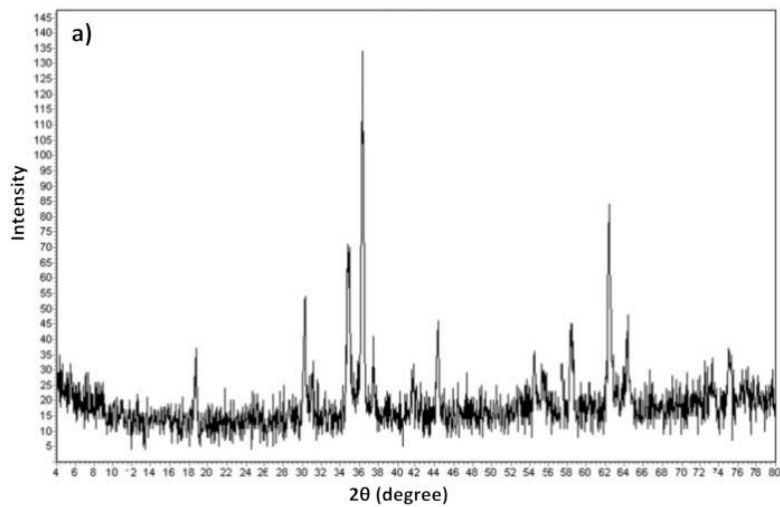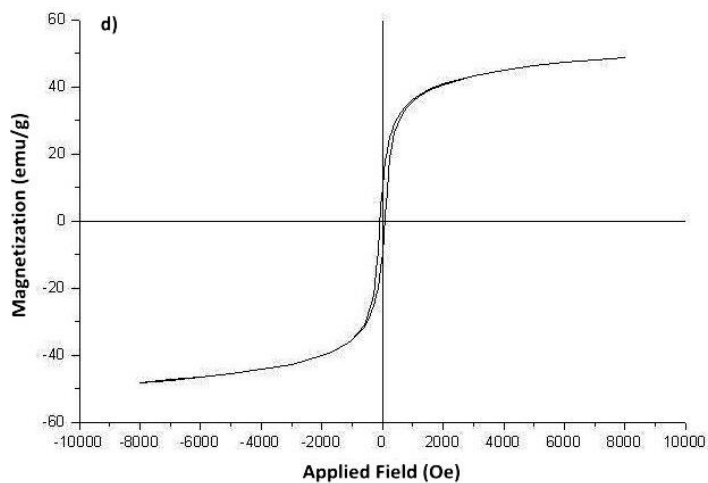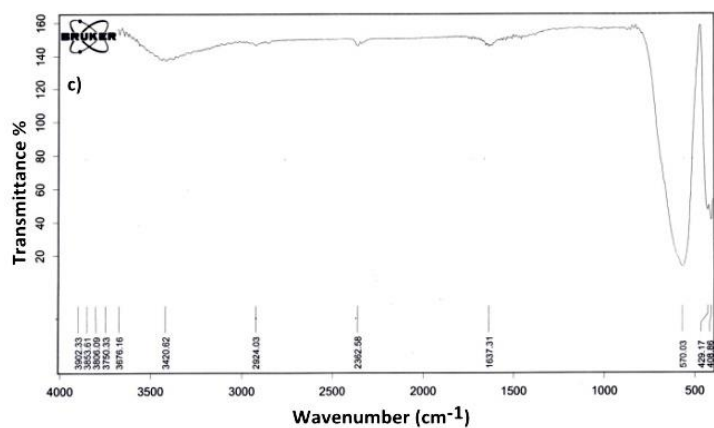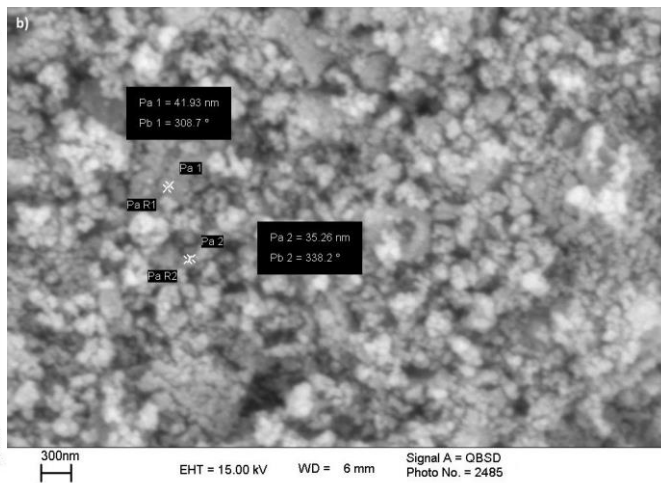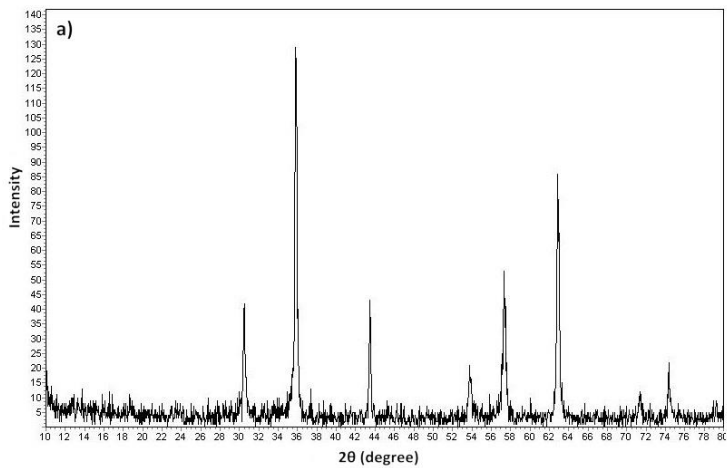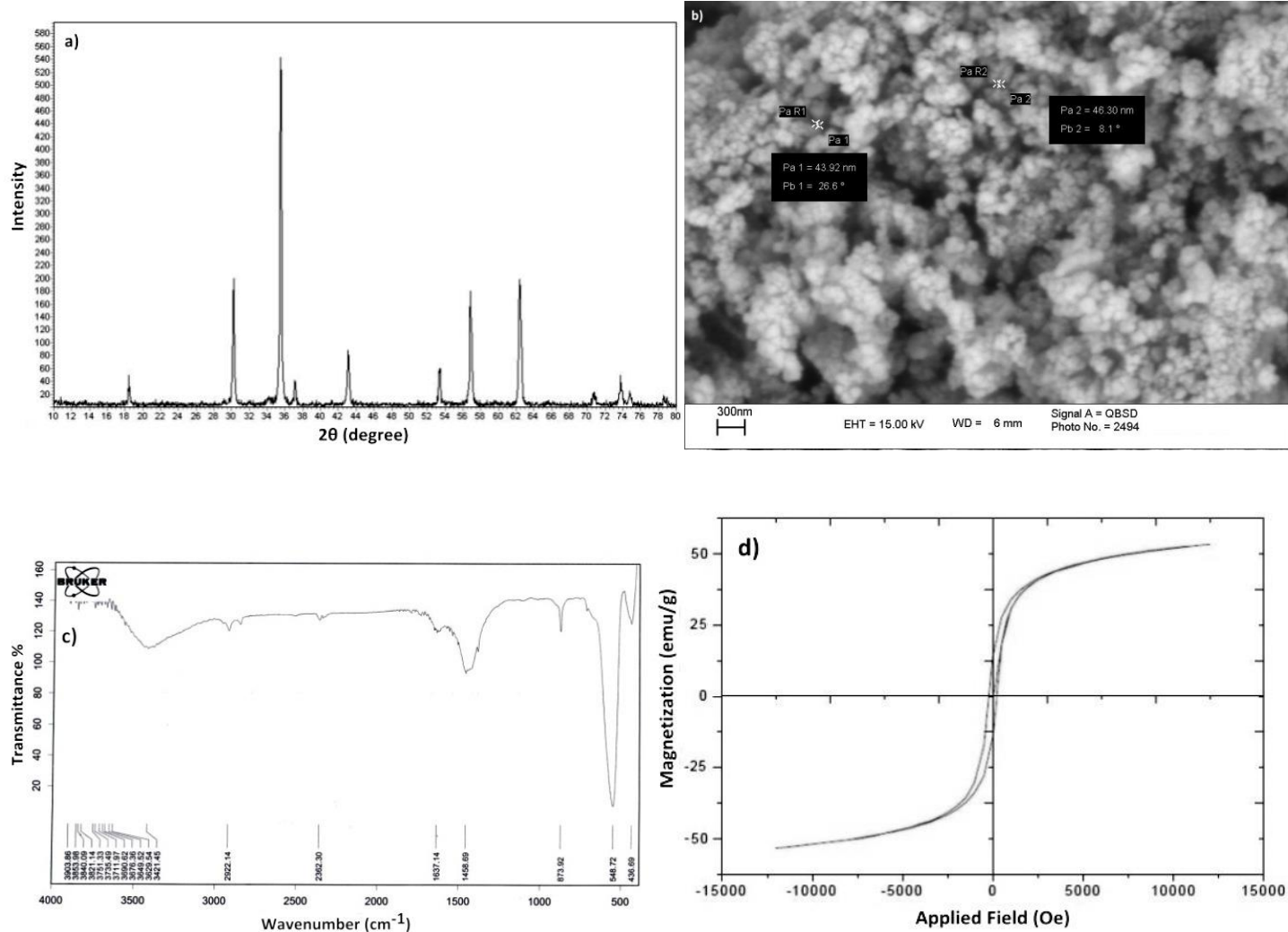
Figure S7. a) X-ray diffraction, b) TEM image and c) FT-IR (KBr) spectrum of $CuFe_2O_4$ MNP.
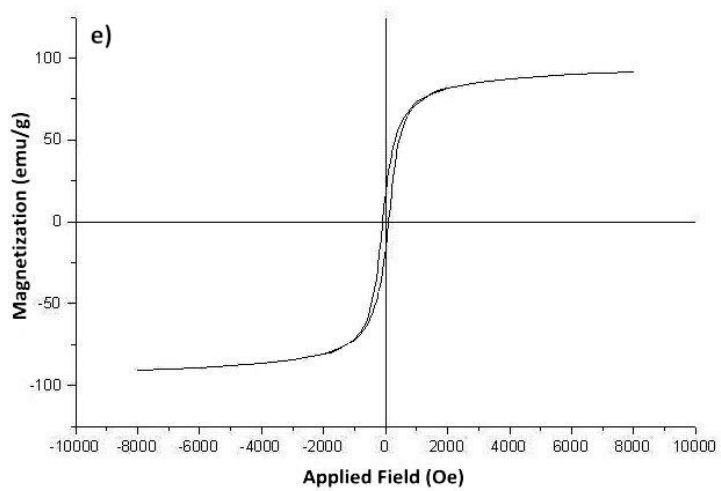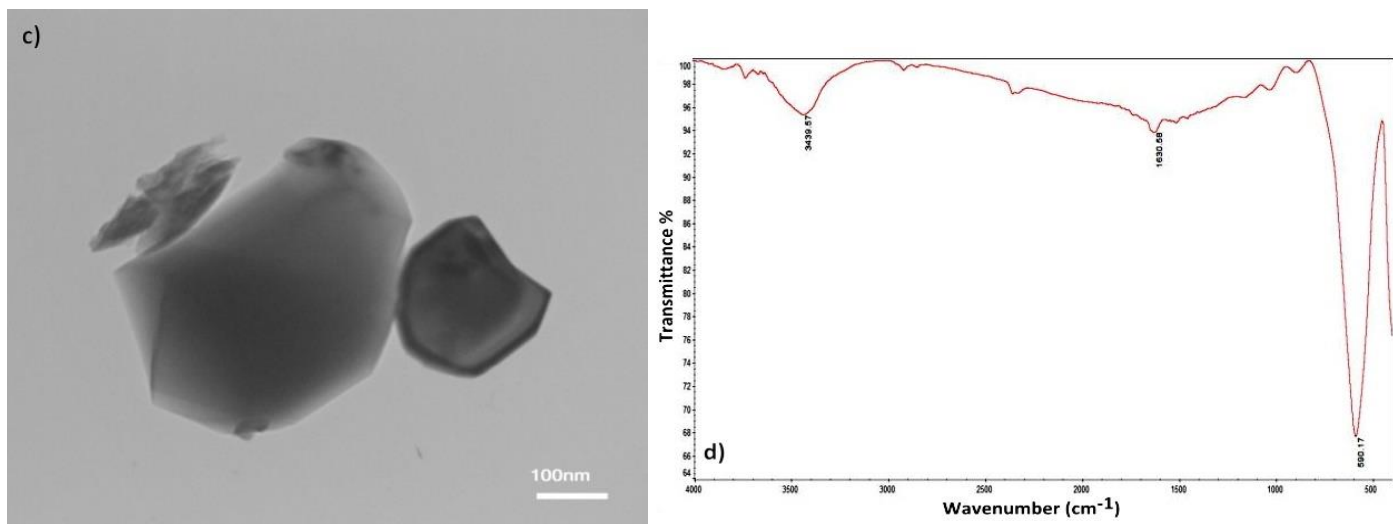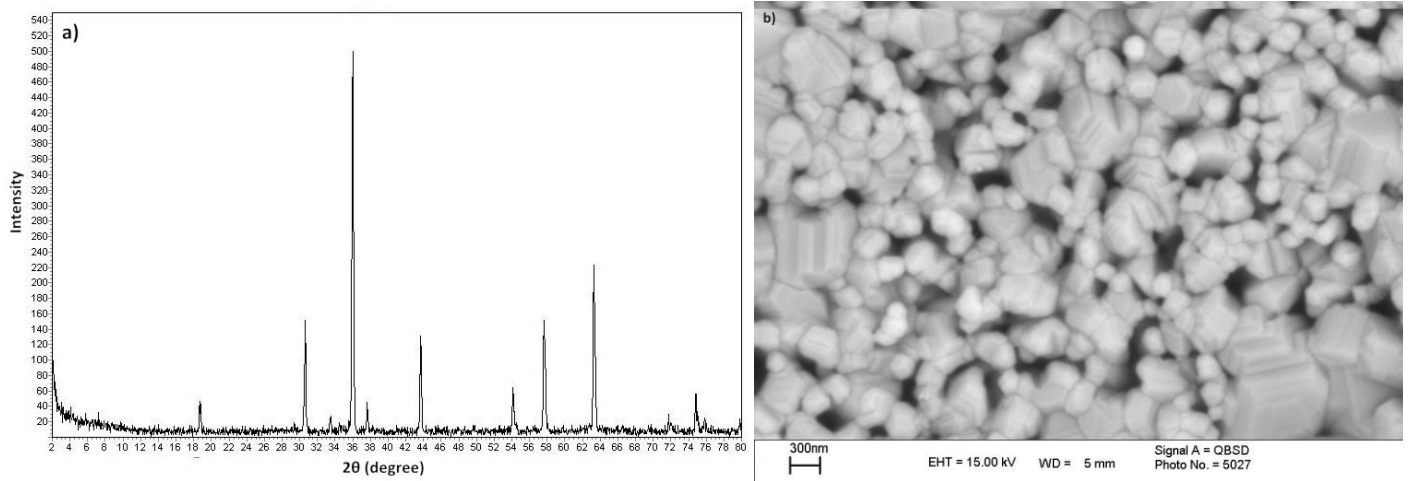
Figures S8. a) X-ray diffraction, b) SEM image, c) TEM image, d) FT-IR (KBr) spectrum, and e) magnetization curve of NiFe$_2$O$_4$ MNPs.

Figures S9. a) X-ray diffraction, b) SEM image, c) FT-IR (KBr) spectrum, and d) magnetization curve of $MgFe_2O_4$

MNPs.

Figures S10. a) X-ray diffraction, b) SEM image, c) FT-IR (KBr) spectrum, and d) magnetization curve of $ZnFe_2O_4$ MNPs.